RESEARCH REPORTS
Biomaterials & Bioengineering

W. Oh[1]*, N. Götzen[2], and K.J. Anusavice[3]

[1]Department of Prosthodontics, College of Dentistry, Health Science Tower, PO Box 100435, University of Florida, Gainesville, FL 32610-0435, USA; [2]Biomechanics Section, Technical University Hamburg-Harburg, Germany; and [3]Department of Dental Biomaterials, College of Dentistry, University of Florida, USA; *corresponding author, woh@dental.ufl.edu

J Dent Res 81(9):623-627, 2002

Influence of Connector Design on Fracture Probability of Ceramic Fixed-partial Dentures

ABSTRACT

Fracture of ceramic fixed-partial dentures (FPDs) tends to occur in the connector area because of stress concentrations. The objective of this study was to test the hypothesis that the radius of curvature at the gingival embrasure of the FPD connector significantly affects the fracture resistance of three-unit FPDs. Two three-dimensional finite element models (FEMs), representing two FPD connector designs, were created in a manner corresponding to that described in a previous experimental study (Oh, 2002). We performed fractographic analysis and FEM analyses based on CARES (NASA) post-processing software to determine the crack initiation site as well as to predict the characteristic strength, the location of peak stress concentrations, and the risk-of-rupture intensities. A good correlation was found between the experimentally measured failure loads and those predicted by FEM simulation analyses. Fractography revealed fracture initiation at the gingival embrasure, which confirms the numerically predicted fracture initiation site. For the designs tested, the radius of curvature at the gingival embrasure strongly affects the fracture resistance of FPDs.

KEY WORDS: ceramic FPD, finite element analysis, fractography, Weibull analysis, risk-of-rupture intensity.

Received August 3, 2001; Last revision April 17, 2002; Accepted June 17, 2002

INTRODUCTION

Stress distributions in a clinical prosthesis can be quite complex. They can consist of compressive, tensile, shear, or mixed stress patterns under typical conditions (Anusavice, 1996; Abu-Hassan *et al*., 1998). Brittle materials, such as dental ceramics, are weak when exposed to tensile stresses (Peterson *et al*., 1998). Therefore, tensile stress is generally considered as a meaningful variable for the assessment of ceramic materials relative to their service life, especially in the presence of flaws. In three-unit ceramic fixed-partial dentures (FPDs), the connector area can be considered as a fracture risk factor, which can increase the tensile stress concentration under flexural compressive loading (Inglis, 1913). The failure rate of three-unit ceramic FPDs around connector areas between retainers and pontics has been reported to be relatively high, especially with the sharper connectors (Kelly *et al*., 1995; Sorensen *et al*., 1999). If the connector design is altered in regions where maximum tension occurs, the characteristic stress pattern can be optimized to improve the survival time of three-unit FPDs. The results of other studies suggest that stresses are better distributed with broadly curved connectors than through the use of more sharply curved connector geometries (Hojjatie and Anusavice, 1990; Kamposiora *et al*., 1996; Pospiech *et al*., 1996). However, specific dimensional limits and sensitivity analyses were not performed.

A prediction of the survival times for ceramic prostheses can be obtained by well-designed prospective clinical trials; however, prosthesis designs are variable, and it is difficult to standardize the designs to ensure realistic estimates of survival times as a function of shape parameters. Model tests with actual ceramic specimens fabricated to the anatomic configuration of teeth may be a useful tool for the identification of their behavior (Kern *et al*., 1993; Koutayas *et al*., 2000). Once the mean loads to failure of prostheses are determined, these data can be applied in mathematical equations to analyze the characteristic strength of the restorations. These invaluable data may reduce the failure probability of ceramic restorations that are controlled by multiple flaws, which cause ceramic structures to fail at stress levels far below their expected strength (Griffith, 1920).

In a previous study, Oh and Anusavice (2002) tested 10 ceramic FPDs for each of 4 connector designs of three-unit ceramic FPDs made of an experimental lithia-disilicate-based core ceramic (VP, batch #1989, Universal shade, Ivoclar AG, Schaan, Liechtenstein), 4 mm in height and 5 mm in width. The core ceramic frameworks were pressed at a temperature of 910°C for 20 min under a pressure of 5 bars. The connector designs were based on the following radii of curvature at the occlusal embrasure (OE) and gingival embrasure (GE): Design I, OE, 0.90 mm and GE, 0.90 mm; Design II, OE, 0.90 mm and GE, 0.25 mm; Design III, GE, 0.25 mm and GE, 0.90 mm; and Design IV, OE, 0.25 mm and GE, 0.25 mm. The FPD specimens were cemented with a resin-based composite on epoxy dies, and compressively loaded axially with a 14.3-mm-diameter steel bearing at the center of the pontic at a crosshead speed of 0.5 mm/min until failure

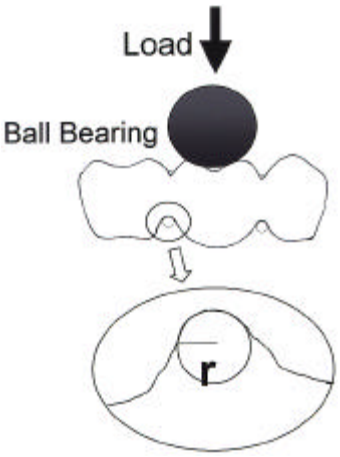

Figure 1. Schematic illustration of axial compressive loading at center of pontic through steel bearing (14.3 mm in diameter) and radius of curvature (r) at embrasure area of three-unit FPDs.

occurred (Fig. 1). Mean loads to failure in each design were obtained and analyzed. However, the fracture origin was not identified.

Fractography is a well-established method for determining the sites of fracture origin that are the most likely areas for clinical failure (Kelly *et al*., 1990, 1995; Thompson *et al*., 1994; Mecholsky, 1995). The stress distribution, failure strength, failure probability, and survival probability of FPD designs can also be estimated by finite element analyses (FEA) based on CARES/ Life post-processing software (Nemeth *et al*., 1990). The fracture-initiating flaw sites may or may not be coincident with the highest stress concentration areas in a geometric morphology. The objectives of the present *in vitro* study were: (1) to determine the magnitude and sensitivity of connector design on the fracture resistance of three-unit all-ceramic FPDs; (2) to identify the flaw origins and crack propagation modes; (3) to compare the experimental failure stresses as a function of design with those obtained from finite element stress analysis models; and (4) to estimate the structural reliability of two FPD designs.

MATERIALS & METHODS

Fractography

The 40 failed pairs of three-unit FPDs specimens from our previous study (Oh and Anusavice, 2002) were collected and stored in a clean environment for fractography for the identification of crack origin, the direction of crack propagation, and the mode of failure. All of the fracture surfaces were cleaned in an ultrasonic bath, palladium-coated, and examined at low magnification (30X), then at higher magnification (70X) under an optical microscope with the aid of a fiber-optic light. Some of the representative specimens were further analyzed by scanning electron microscopy (SEM) (JSM 6400, Jeol, Peabody, MA, USA).

Finite Element Analyses

Two three-dimensional finite element models of a three-unit all-ceramic FPD were created. Since a three-unit FPD exhibits an approximate symmetry with respect to the central pontic, only half of the structure was modeled (Fig. 2A). The models were meshed entirely with higher-order brick and shell elements. Ceramic and epoxy resin were selected to simulate linearly elastic materials. The periodontal ligament and the resin-bonding layer were not modeled.

All connectors were 4 mm in height and 5 mm in width. Two radii of curvature at the gingival embrasure were designed: Model I, 0.45 mm, and Model II, 0.25 mm. Since the previous experimental study found no statistically significant effect of occlusal embrasure radius on the fracture resistance of the ceramic FPD, the occlusal embrasures for Models I and II were prepared with an identical sharp-notch design. A radius of 0.45 mm was selected rather than a radius of 0.90 mm at the gingival embrasure for Model I to maintain connector height constant at 4 mm without altering the curvature at the gingival embrasure. Thus, simulation Model I and Model II were matched with the designs of experimental Groups A (Designs I and III: radius of the GE, 0.90 mm) and B (Designs II and IV: radius of the GE, 0.25 mm), respectively.

A simulated load of 100 N was applied at the central fossa of the pontic. This loading configuration induced maximum bending stress in the prostheses. The load was distributed uniformly over the plane of symmetry (central cross-section of the pontic) through the use of coupling equations. This option was chosen to minimize any Hertzian contact stresses, which would increase the localized stress and may cause local chipping of a ceramic, and that would yield erroneous results in the simulation analysis. Horizontal displacement of all nodes belonging to the plane of symmetry was constrained to create symmetrical boundary conditions. Linear elastic stress analyses were performed with the ANSYS FEA software to determine the stress distribution within the ceramic and to identify the regions where peak stresses occur.

Reliability Estimation

The FEA post-processing software, NASA CARES/Life, developed by Nemeth *et al*. (1990), was used for estimation of the characteristic strength of the 4 FPD designs. It uses numerically determined stress results from FEA in combination with fracture statistics, including the two-parameter Weibull function and Batdorf theory, to predict the fracture reliability of isotropic ceramic components. We determined the characteristic strength of the 2 FPD designs by computing the applicable load for a given fracture failure probability of 63.2%. We performed non-linear curve-fitting through a least-squares method to obtain Weibull parameters for comparison of characteristic strength values obtained from the simulation analyses. We also calculated maximum stress values by incorporating the experimental characteristic strength values into the simulation models. Risk-of-rupture intensities (RRI) were evaluated for each finite element model design at its experimental failure load. We identified the most likely fracture initiation site within each FPD by plotting the contours of these intensity values.

Statistical Analyses

Weibull analyses were performed with the experimentally measured load-at-failure values for each FPD design. These analyses yielded the experimentally determined characteristic strength values (63.2% failure probability) associated with each design. The results were then compared with the numerically determined characteristic strength values.

RESULTS

Fractography

The fracture origin was detected at the gingival embrasure in all samples (Fig. 1B). On the lustrous fracture surface, velocity hackle patterns consistently converged toward the semilunar area. Pores were more concentrated at the gingival embrasure areas, and some of the flaws related to multiple pores, ranging

from 10 to 60 μm in diameter (Fig. 1C). The greatest probabilities for crack origin sites within the gingival embrasure were as follows: (1) 67.5% in the buccolingual plane at the center, and (2) 53% in the mesiodistal plane at abutment crowns (Table 1).

Finite Element Model Analysis

Two sites of severe stress concentrations were identified. Peak compressive stresses occurred at the occlusal embrasure, and peak tensile stresses developed at the gingival embrasure, either at the center or at a position shifted slightly buccally. The peak tensile stress, under a unit load of 100 N, was higher, with the smaller radius of curvature at the gingival embrasure: Model II revealed a higher peak tensile stress (21.0 MPa) than Model 1 (16.1 MPa) (Table 2).

Reliability Estimation

The Weibull moduli (m) were 6.3 for Group A and 8.6 for Group B. The characteristic strength values for experimental Groups A and B were 987 N and 735 N, respectively. These values were comparable with the values of 1031 N and 740 N for simulation Models I and II, respectively (Table 2). The maximum tensile stress values under loads associated with values of characteristic strength values are also summarized in Table 2. The distribution of typical risk-of-rupture intensity values computed for each design under its failure load is shown in Fig. 1D. Peak intensity sites were found close to the apex of the gingival embrasure curvature, and were shifted slightly toward the pontic. This result may be predictive of the most probable site of fracture initiation leading to failure of these FPD designs.

Table 1. Fracture Origin Locations at the Embrasures (The percentages of fractured ceramic specimens are denoted.)

	Occlusogingival Location		Buccolingual Location			Mesiodistal Location		
Designs	OE[a]	GE[b]	Buccal	Central	Lingual	Abutment	Center	Pontic
I	0.0	25.0	0.0	17.5	7.5	12.5	7.5	7.5
II	0.0	25.0	7.5	12.5	5.0	12.5	5.0	2.5
III	0.0	25.0	5.0	17.5	2.5	15.0	7.5	5.0
IV	0.0	25.0	2.5	20.0	2.5	12.5	7.5	2.5
Subtotal	0.0%	100.0%	5.0%	67.5%	17.5%	52.5%	30.0%	17.5%
Total no. of specimens	40		40			40		

[a] OE = occlusal embrasure.
[b] GE = gingival embrasure.

Table 2. Summary of Characteristic Strength, Peak Stress, Maximum Stress, and Weibull Modulus Values for Each Simulation Model (I and II) and Experimental Group (A and B)

Model	Characteristic Strength Value (N)		Peak Tensile Strength Value	Maximum Tensile Strength Value	Weibull Modulus	
(Group)	EDV[a]	MPV[b]	(MPa)	(MPa)	EDV	MPV
I (A)	987	1031	16.1	165	6.3	8.6
II (B)	735	740	21.0	155	8.6	8.6

[a] EDV = experimentally determined value.
[b] MPV = mathematically predicted value.

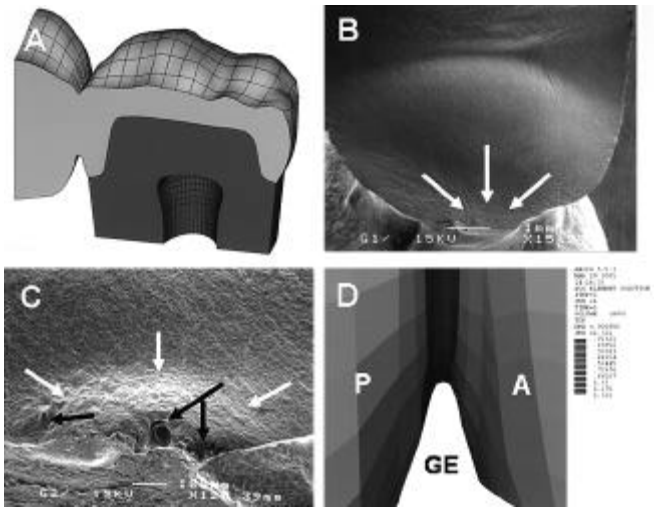

Figure 2. Finite element model (FEM) and scanning electron microscopic (SEM) images: **(A)** cross-sectional view of longitudinally sectioned 3-D FEM Model II, **(B)** SEM image of a typical fracture surface of a failed ceramic specimen, **(C)** SEM image of a flaw origin (indicated by white arrows) and adjacent multiple pores (indicated by black arrows) at the gingival embrasure, and **(D)** contour plot of the risk-of-rupture intensity (RRI) for FPD Model II at a failure load of 740 N. Peak intensity site at the gingival embrasure is slightly shifted toward the pontic. The gingival embrasure, pontic, and abutment crown are denoted as GE, P, and A, respectively.

DISCUSSION

The morphology of the connector design at the gingival embrasure is critical in reducing the fracture probability in the experimental test specimens, and these results are consistent with those yielded from the mathematical (FEA) analyses. Model I, having a larger radius of curvature at the gingival embrasure, exhibited a lower tensile stress concentration at the gingival embrasure, compared with Model II. This is in agreement with a previous finding of greater stress concentration within the connector, and the stress concentration was greater for a reduced height and a broader connector width for FPDs (Kelly *et al*., 1995; Kamposiora *et al*., 1996; Pospiech *et al*., 1996). In the present study, an axial force applied at the center of pontic in a three-unit FPD

produced a compressive stress distribution pattern within the prosthesis at the occlusal embrasure and a tensile stress distribution at the gingival embrasure, supporting the theoretical concept proposed by Anusavice (1996). Considering the fracture susceptibility of ceramic prosthesis to tensile stress, this finding is useful for designing three-unit ceramic FPDs (Peterson *et al*., 1998). The fracture resistance can be improved by increasing the radius of curvature at the gingival embrasure of the FPD without affecting esthetics by keeping the occlusal embrasure as sharp as possible.

Present fractographic analyses revealed that the failure origin of the three-unit ceramic prosthesis occurred at the gingival embrasure in all specimens, supporting the FEA model prediction of the highest tensile stress concentration at the gingival embrasure. This finding is consistent with a previous study of retrieved clinical ceramic three-unit FPDs in which all cracks initiated in the connector region (Kelly *et al*., 1995). In our study, cracks propagated from the gingival embrasure toward the occlusal loading on pontic. The fracture origin was most common at the center of the gingival embrasure in a buccolingual dimension, and it was shifted slightly toward the margin area of the abutment crown in a mesiodistal direction. In some of the samples, adjacent margins were chipped or fractured, breaking the cement seal. This finding supports a suggestion that the ceramic be reinforced at the proximal margin area. Interestingly, the stress distribution pattern in simulation models was not consistent with the failure patterns found in the experimental study: The peak intensity shifted slightly to the pontic side (Fig. 2D). This finding does not necessarily invalidate the failure of ceramic prostheses within the pontic area because of the differential thickness of ceramic material. The thickness at the proximal margin was only 1 mm. Nonetheless, a typical beam-bending situation occurred in the three-unit FPDs because the more sharply curved gingival embrasure acted as a macroscopic flaw. Once microcracks initiate at the gingival embrasure under the tensile stress concentration, they continue to grow, with a repetitive plastic blunting and sharpening process at the crack tip under a dominant Mode I compressive load, until bulk failure of the ceramic prosthesis occurs (Frechette, 1990).

Different sizes (from 10 to 60 μm) of pores were concentrated around the flaw site, indicating a strong relationship with the reduced fracture resistance of the FPDs (Koseyan and Biswas, 1976; Thompson *et al*., 1994; Abu-Hassan *et al*., 1998) (Fig. 2C). However, the pores were well-rounded, and they were associated with reduced stress concentrations, compared with irregular pores found in underfired aluminous porcelain (Piddock, 1989). The more spherical pores found in our study suggest a relatively lower glass viscosity for the ceramic. Greater stress concentration may also be affected by the sprue design or the processing technique itself. Thermal differences experienced during processing may generate volume changes of the ceramic, leading to formation of pores (Khajotia *et al*., 1999). Sprues were connected on the central fossa of each abutment crown, extending vertically to a runner bar. This effect requires further study.

The Weibull failure probability can be used to predict the service lifetime of intrinsically brittle materials, such as ceramic ceramics, by calculating the risk of failure as a function of time (Kelly *et al*., 1995; Tinschert, 2000). Weibull moduli for the ceramic restorations ranged from 6.3 to 8.6, which was consistent with the value reported for In-ceram core ceramic (m = 6.7) (Kelly *et al*., 1995). The probability of failure based on FEA corresponds well with the experimental values. The numerically calculated characteristic strength values were slightly higher than the experimental values by a factor of only ± 5%. This finding supports the case of the mathematical model and the experimental *in vitro* model, and also indicates that NASA CARES software is potentially useful for estimating the strength characteristics and survival probabilities of three-unit ceramic FPDs.

Based on the conditions of this study, the following conclusions are proposed: (1) The radius of curvature at the gingival embrasure strongly affects the fracture resistance of all-ceramic FPDs, (2) fracture mechanics principles can provide critically important information for the identification of sensitive design factors and probable fracture sites in clinical prostheses, and (3) NASA CARES software used as an adjunct to FEA is useful for the optimization of prosthesis designs.

ACKNOWLEDGMENTS

This paper was presented at the IADR General Session, Chiba, Japan, June, 2001. Dr. Oh was the recipient of the 2001 Frechette Award. This study was supported by NIH-NIDCR Grant No. DE06672.

REFERENCES

Abu-Hassan MI, Abu-Hammad OA, Harrison A (1998). Strains and tensile stress distribution in loaded disc-shaped ceramic specimens. An FEA study. *J Oral Rehabil* 25:490-495.

Anusavice KJ (1996). Phillips' science of dental materials. 10th ed. Philadelphia: W.B. Saunders, pp. 50-53.

Frechette VD (1990). Failure analysis of brittle materials. *Adv Ceram* 28:46-59.

Griffith AA (1920). The phenomena of rupture and flow in solids. *Philos Trans R Soc Lond Series A* 221:163-198.

Hojjatie B, Anusavice KJ (1990). Three-dimensional finite element analysis of glass-ceramic dental crowns. *J Biomech* 23:1157-1166.

Inglis CE (1913). Stresses in a plate due to the presence of cracks and sharp corners. *Trans Inst Naval Archit* 55:219-241.

Kamposiora P, Papavasiliou G, Bayne SC, Felton DA (1996). Stress concentration in all-ceramic posterior fixed partial dentures. *Quintessence Int* 27:701-706.

Kelly JR, Giordano R, Pober R, Cima MJ (1990). Fracture surface analysis of dental ceramics: clinically failed restorations. *Int J Prosthodont* 3:430-440.

Kelly JR, Tesk JA, Sorensen JA (1995). Failure of all-ceramic fixed partial dentures *in vitro* and *in vivo*: analysis and modeling. *J Dent Res* 74:1253-1258.

Kern M, Douglas WH, Fechtig T, Strub JR, DeLong R (1993). Fracture strength of all-porcelain, resin-bonded bridges after testing in an artificial oral environment. *J Dent* 21:117-121.

Khajotia SS, Mackert JR Jr, Twiggs SW, Russell CM, Williams AL (1999). Elimination, via high-rate laser dilatometry, of structural relaxation during thermal expansion measurement of dental porcelains. *Dent Mater* 15:390-396.

Koseyan GK, Biswas CP (1976). A study of ceramic-metal restoration process. *J Prosthet Dent* 36:694-698.

Koutayas SO, Kern M, Ferraresso F, Strub JR (2000). Influence of design and mode of loading on the fracture strength of all-ceramic

resin-bonded fixed partial dentures: an in vitro study in a dual-axis chewing simulator. *J Prosthet Dent* 83:540-547.

Mecholsky JJ Jr (1995). Fractography: determining the sites of fracture initiation. *Dent Mater* 11:113-116.

Nemeth NN, Manderscheid JM, Gyekenyesi JP (1990). Design of ceramic components with the NASA/CARES computer program. NASA TM-102369; NASA Lewis Research Center.

Oh W, Anusavice KJ (2002). Effect of connector design on fracture resistance of all-ceramic fixed partial dentures. *J Prosthet Dent* 87:536-542.

Peterson IM, Pajares A, Lawn BR, Thompson VP, Rekow ED (1998). Mechanical characterization of dental ceramics by Hertzian contacts. *J Dent Res* 77:589-602.

Piddock V (1989). Effect of alumina concentration on the thermal diffusivity of dental porcelain. *J Dent* 17:290-294.

Pospiech P, Rammelsberg P, Goldhofer G, Gernet W (1996). All-ceramic resin-bonded bridges. A 3-dimensional finite-element analysis study. *Eur J Oral Sci* 104:390-395.

Sorensen JA, Cruz M, Mito WT, Raffeiner O, Meredith HR, Foser HP (1999). A clinical investigation on three-unit fixed partial dentures fabricated with a lithium disilicate glass-ceramic. *Pract Periodont Aesthet Dent* 11:95-106.

Thompson JY, Anusavice KJ, Naman A, Morris HF (1994). Fracture surface characterization of clinically failed all-ceramic crowns. *J Dent Res* 73:1824-1832.

Tinschert J, Zwez D, Marx R, Anusavice KJ (2000). Structural reliability of alumina-, feldspar-, leucite-, mica- and zirconia-based ceramics. *J Dent* 28:529-535.